infrastructures

MDPI

Article

A Modified Catenary Model with Application to the Analysis and Design of Retrofit Cables for Progressive Collapse

Leven T. Deputy, Yasha Zeinali and Brett A. Story *

Department of Civil and Environmental Engineering, Bobby B. Lyle School of Engineering, Southern Methodist University, Dallas, TX 75275, USA; ldeputy@smu.edu (L.T.D.); yhajizeinali@smu.edu (Y.Z.)
* Correspondence: bstory@smu.edu; Tel.: +1-214-768-1991

Received: 28 June 2018; Accepted: 17 July 2018; Published: 20 July 2018

Abstract: Progressive collapse, the extensive or complete collapse of a structure resulting from the failure of one or a small number of structural components, has become a focus of research efforts and design considerations following events occurring at the Ronan Point apartment building in London, the Murrah Federal Building in Oklahoma City, and the World Trade Center in New York City. A principle research and design area for progressive collapse investigates the behavior of structural frames when column support is removed. The mechanism that results from loss of column support in structural frames characteristically involves beams that are unable to provide sufficient flexural resistance. Cable retrofit is one method to enhance existing frames and supplement or replace the post-mechanism beam load resistance with straight-legged catenary resistance after a column removal. The cables are located linearly along the beam geometry and are affixed at beam supports. This paper investigates both static and dynamic behavior of the catenary action of retrofit cables, which include both the linear and nonlinear material behavior of the cable material. Moreover, a simplified model serves as the basis for retrofit cable design is presented. Finite element modeling and experimentation in this paper verify and validate the applicability of the model. Finally, a framework for developing a procedure for retrofit cable design is presented.

Keywords: progressive collapse; disproportionate collapse; catenary action; non-linear analysis; cable retrofit; modified catenary

1. Introduction

Catenary behavior plays a significant role in the behavior of structural elements resisting loads capable of causing progressive collapse [1–6]. Members designed to resist primarily flexural action in frame structures can undergo significant catenary action under column loss scenarios in both steel [7,8] and concrete [9–12] systems. For example, in an interior column loss scenario shown in Figure 1, span lengths are effectively doubled and subjected to significant load increases from the columns above over a very short time. The flexural capacity of the beams is likely inadequate to solely support the dynamic load, thus mechanisms occur at supports, and alternative resistance paths (e.g., catenary action from frame members or additional retrofit cables) are required to achieve equilibrium and avoid progressive collapse. The transition from flexural resistance to catenary resistance has been observed in experimental work comprising static application of load to structural systems of different materials [13–22]. The ultimate structural resistance in column removal is a form of catenary behavior that may be available in the frame itself and can also be provided through the use of retrofitted cables. Unlike many geometrically linear structural components (e.g., beams, trusses), catenary systems exhibit non-linear load-displacement relationships. Thus, linear structural analysis techniques for

characterizing load-deflection relationships are not applicable. For example, in instances of "small" initial variations from horizontal (i.e., shallow modified catenary), truss analysis is not appropriate and nonlinear geometry must be considered. Forms of this shallow modified catenary can be seen in several structural applications: progressive collapse retrofit [23,24], progressive collapse resisted by concrete reinforcement [9,20], overhead wires for electric rail [25,26], and ice loads and wind-on-ice loads on electrical power lines [27,28].

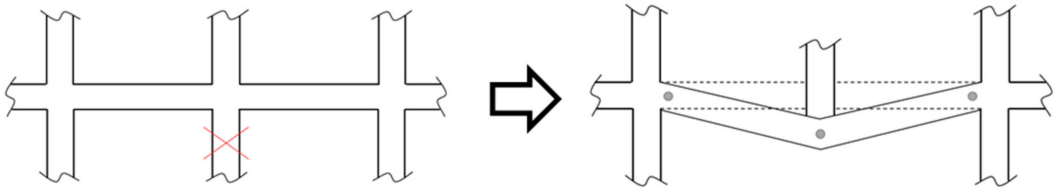

Figure 1. Idealized column removal scenario.

This paper investigates fundamental modified catenary (M.C.) behavior and presents a preliminary model that describes the static and dynamic nonlinear catenary behavior of structural elements with minimal flexural stiffness, for example, retrofit cables. Cables attached at column supports and along the beam can be used to provide or supplement load carrying capacity under loss of column support conditions [23,24,29,30]. Upon loss of column support, the beam and cable initially resist load in tandem according to the existing capacity of the beam and its connections. For simplicity in design, this paper assumes that the retrofit cable is required to transfer the entire load.

This (M.C.) model provides a fundamental understanding of the stiffness of the catenary throughout the static load-deflection behavior and incorporates this stiffness in nonlinear dynamic analyses. The model is validated with finite element simulations and small-scale cable experiments in which static and dynamic loads are applied to cables. Loading scenarios within and beyond the elastic range of the cable material are considered. Lastly, an illustrative application of the M.C. model cable retrofit design is presented.

2. Modified Catenary Behavior

The true catenary shape forms when a structural span with negligible flexural stiffness (i.e., a cable) is subject to uniform self-weight. A modified version of the catenary form occurs when a span with negligible flexural stiffness is subject to a point load from a concentration of mass (Figure 2). The amount of mass concentrated at the midspan is assumed to be the dominant loading and the self-weight of the modified catenary itself is assumed to be relatively small. These assumptions apply in progressive collapse scenarios in which a floor is responsible for large column forces from one or more floors [10,12,15,18]. Boundary conditions are idealized as frictionless pins that offer no moment resistance. Material constitutive relationships are assumed as elastic–perfectly plastic. Two important assumptions for both general analytical modeling and cable retrofit design in this paper are (a) adjoining spans are equal in length, cross-section, and material properties; and (b) the end supports do not translate laterally. Even small lateral movements, such as spring-type action of columns moving laterally because of the horizontal catenary forces, can have a significant impact on results.

2.1. Load-Deflection Equations

The load-deflection relationship for the modified catenary is derived from the geometry and dynamic equilibrium of forces in Figure 2 [31]. In this analysis, m represents an effective, concentrated mass acted upon by gravity, g. The variables δ_0, θ_0, L_0, and s are the initial vertical displacement, the undeformed slope, undeformed span length, and the horizontal projection of L_0, respectively. The deformed span length, L, experiences tension, T, over cross-sectional area, A. The variables u and θ are the vertical displacement and slope of the deformed modified catenary, respectively. The material

behavior for the M.C. model is defined by the elastic and inelastic regimes of an elastic–perfectly plastic model. The variables E and F_y define the material properties in these regimes; damping is not considered. Dynamic equilibrium on the mass in Figure 2 results in the following equation of motion:

$$\sum F_y = m\ddot{u} \Longrightarrow -2Tsin\theta + mg = m\ddot{u} \tag{1}$$

Geometric relationships in terms of the vertical displacement, u, are as follows:

$$L = \sqrt{(\delta_0 + u)^2 + s^2} \tag{2}$$

$$\sin\theta = \frac{\delta_0 + u}{\sqrt{(\delta_0 + u)^2 + s^2}} \tag{3}$$

$$\Delta = L - L_0 = \frac{TL_0}{EA} \tag{4}$$

The tensile force is defined by the following piecewise relationship:

$$T = \begin{cases} \frac{EA}{L_0}\left(\sqrt{(\delta_0 + u)^2 + s^2} - L_0\right) & \Delta \leq \Delta_y \\ AF_y & \Delta > \Delta_y \end{cases} \tag{5}$$

After combing Equations (1)–(5), the equation of motion for the nonlinear elastic system is as follows:

$$m\ddot{u} = \begin{cases} -2\frac{EA}{L_0}\left(\sqrt{(\delta_0 + u)^2 + s^2} - L_0\right)\frac{\delta_0 + u}{\sqrt{(\delta_0 + u)^2 + s^2}} + mg & \Delta \leq \Delta_y \\ -2AF_y\frac{\delta_0 + u}{\sqrt{(\delta_0 + u)^2 + s^2}} + mg & \Delta > \Delta_y \end{cases} \tag{6}$$

For the static case, replacing the gravity force with a general concentrated force, P:

$$P = \begin{cases} 2\frac{EA}{L_0}\left(\sqrt{(\delta_0 + u)^2 + s^2} - L_0\right)\frac{\delta_0 + u}{\sqrt{(\delta_0 + u)^2 + s^2}} & \Delta \leq \Delta_y \\ 2AF_y\frac{\delta_0 + u}{\sqrt{(\delta_0 + u)^2 + s^2}} & \Delta > \Delta_y \end{cases} \tag{7}$$

The static load-displacement relationship is shown in Figure 3; geometrically non-linear behavior occurs in the elastic range. Equations (6) and (7) have no restrictions on the values of δ_0 or u. For small initial deflections, the resulting load-deflection relationship is nonlinear. Previous research and analysis of catenary behavior in progressive collapse has addressed the catenary behavior for larger δ_0 values [11,18].

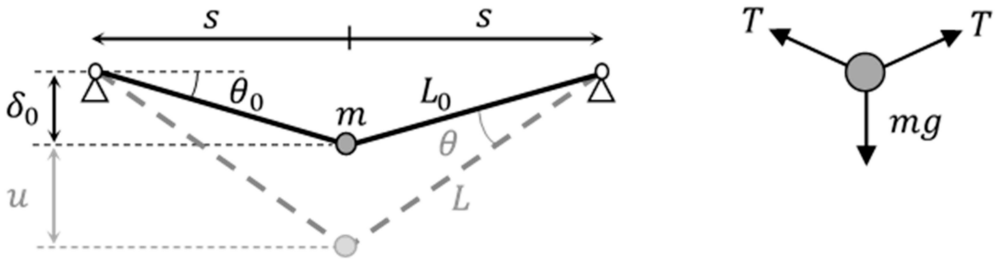

Figure 2. Modified catenary system.

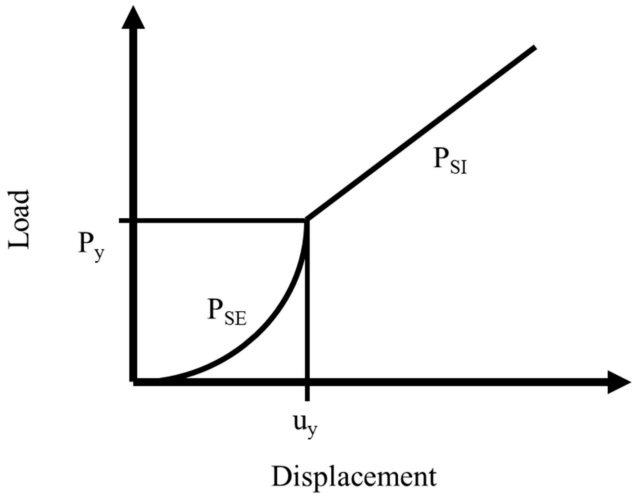

Figure 3. Static load-displacement relationship.

2.2. Approximate Static Load-Deflection Equations for Design

An approximate static load-deflection relationship in the elastic material range can be estimated by rewriting Equation (7) and solving for P_{SE}, which is the applied load at the mid-span (representing, for example, the axial force from the column above):

$$P_{SE} = 2\frac{EA}{L_0}\left(\sqrt{(\delta_0+u)^2+s^2}-L_0\right)\frac{\delta_0+u}{\sqrt{(\delta_0+u)^2+s^2}} \tag{8}$$

Equation (6) can be rewritten as follows:

$$P_{SE} = 2\frac{EA}{L_0}\left(\frac{(\delta_0+u)^2+s^2-{L_0}^2}{\sqrt{(\delta_0+u)^2+s^2}+L_0}\right)\frac{\delta_0+u}{\sqrt{(\delta_0+u)^2+s^2}} \tag{9}$$

Under the assumption that $\delta_0 << s$, $s \approx L_0$, then, $s^2 - {L_0}^2$ is equal to zero, and all L_0 can be replaced by s. So, Equation (9) can be rewritten as follows:

$$P_{SE} = 2\frac{EA}{s^3}\left(\frac{(\delta_0+u)^2}{1+\sqrt{\left(\frac{\delta_0+u}{s}\right)^2+1}}\right)\frac{\delta_0+u}{\sqrt{\left(\frac{\delta_0+u}{s}\right)^2+1}} \tag{10}$$

Extending the assumption further such that the ratio $\frac{\delta_0+u}{s}$ is small, Equation (10) becomes the following:

$$P_{SE} = \frac{EA(\delta_0+u)^3}{s^3} \tag{11}$$

In the inelastic material range, the tensile force in each cable arm becomes the yield force and the static force in the inelastic range, P_{SI}, is as follows:

$$P_{SI} = 2\frac{AF_y(\delta_0+u)}{s} \tag{12}$$

2.3. Dynamic Load Deflection Equations Using Dynamic Amplification Factors

The progressive collapse design process must account for dynamic effects either by direct dynamic analysis or through static analysis and dynamic amplification factors. Dynamic effects produce larger

demand than indicated by static analyses. Therefore, either a dynamic design procedure that directly calculates the required cross-sectional area of steel or a static design procedure that incorporates adjustments for dynamic effects is required. Kunnath et al. [32] provide a summary of energy approaches in progressive collapse applications [32–35]. Utilizing an energy approach relating maximum dynamic response with a static response involves equating internal strain energy with work done by the externally-applied dynamic load; kinetic energy is assumed to be zero initially and at the point of maximum deflection. This energy relationship is shown graphically in Figure 4.

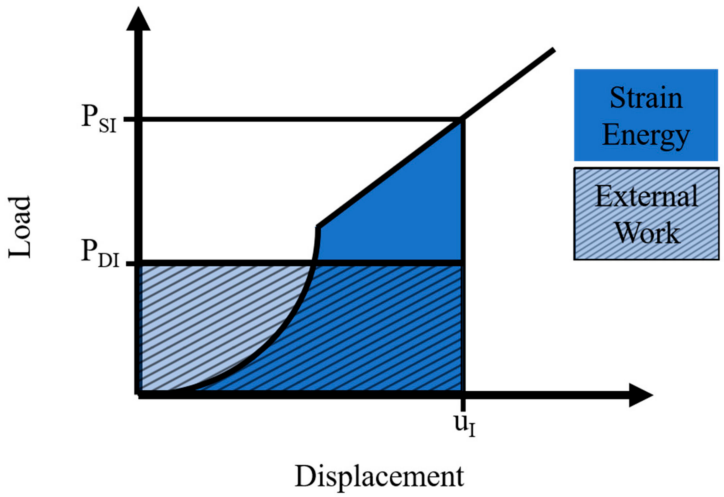

Figure 4. Energy Approach.

For the elastic case, the internal strain energy caused by the static load to a static, elastic displacement, u_{SE}, is equal to the external work done by the dynamic load up to the same elastic deflection:

$$\int_0^{u_{SE}} P_{SE} du = P_{DE} u_{SE} \tag{13}$$

Similarly, for the inelastic case:

$$\int_0^{u_y} P_{SE} du + \int_{u_y}^{u_{SI}} P_{SI} du = P_{DI} u_{SI} \tag{14}$$

From Equation (13), and substituting P_{SE} from Equation (11), the relationship between static and dynamic loads in the elastic range becomes the following:

$$P_{DE} = \frac{E A {u_{SE}}^3}{4S^3} = \frac{P_{SE}}{4} \tag{15}$$

Substituting αu_y for an arbitrary limiting static deflection in the inelastic range, u_{SI}, where $\alpha > 1$, Equation (14) becomes the following:

$$P_{DI} \alpha u_y = \frac{E A u_y^4 + 4S^2 A F_y {u_y}^2 (\alpha^2 - 1)}{4 \alpha S^3} \tag{16}$$

Equating P_{SE} and P_{SI} at u_y provides the following expression for the yield displacement:

$$u_y = s \sqrt{\frac{2F_y}{E}} \tag{17}$$

Substituting Equation (17) into Equation (16) and factoring P_{SI} from Equation (12):

$$P_{DI} = \frac{\left(\alpha^2 - \frac{1}{2}\right)}{2\alpha^2} P_{SI} \tag{18}$$

The amplification factors, β_E and β_I, relating dynamic and static loads in the elastic and inelastic range, respectively, are as follows:

$$\beta_E = \frac{1}{4} \tag{19}$$

$$\beta_I = \frac{\left(\alpha^2 - \frac{1}{2}\right)}{2\alpha^2} \tag{20}$$

The bounds of β_I are ¼ at yield and approach ½ as α increases.

3. Materials, Methods, and Experimental Setup

3.1. Finite Element Model of M.C. System

Numerical verifications of the results from the M.C. model and experiments were carried out in the finite element solver OpenSees (O.S.). The nonlinear finite element model considers corotational geometry transformation using truss elements and elastic–perfectly plastic material behavior. Boundary conditions are pinned at each support and internal hinges are located at the midspan at the location of the load. Displacement control is utilized with an increment of 0.25 mm and a modified Newmark integration method for dynamic analysis. Table 1 provides quantities of interest for small-scale (experiments) and large-scale (design and analysis examples) configurations. The results from the static and dynamic M.C. and O.S. analyses are presented in Section 4.1.

Table 1. Modified Catenary Configuration Properties.

	s (mm)	A (mm^2)	E (GPa)	Fy (MPa)
Configuration 1 (Small Scale)	340	1.5	200	460
Configuration 2 (Large Scale)	6.1×10^3	3.2×10^3	97	830

3.2. Static Experiments

In order to validate the analytical modified catenary model and observe the predicted nonlinear behavior, experimental static tests were performed. A small-scale reaction frame was designed and constructed for use in an INSTRON 5582 axial load frame shown in Figure 5. The reaction frame was designed to prevent translation in the vertical and horizontal directions at the boundaries of each specimen; vertical and lateral stiffnesses of the frame were measured as 380 N/mm and 760 N/mm, respectively. For each small-scale experimental investigation, the test specimen was a 16-gage mild steel wire with the geometric and material properties shown in Table 1; Figure 6 displays the constitutive character of the wire specimens in Configuration 1. The wire was clamped at both ends and subjected to a quasi-static displacement control. The displacement was increased at a constant rate of 0.1 mm/s. Load and deflection data were collected using the INSTRON 5582 load cell and header displacement for comparisons with analytical modified catenary models.

Several different initial deflections and final displacement values were investigated. Each test began at the reference location representing an initial deflection of 0 mm for Test 1. Specimens engaged at the residual deformation from the previous test. Initial deflections of 0 mm (Test 1), 30 mm (Test 2), 30 mm (Test 3), and 52 mm (Test 4) were repeated for the same specimen. The experiments were performed in displacement control comprising a steady loading phase and a two-cycle linear sawtooth unloading and loading phase. In Test 1, the specimen was loaded into the inelastic region to a deflection of 38.1 mm and then unloaded; a residual deformation of 30 mm occurred. In Test 2, the specimen was reloaded and

unloaded elastically from and to this residual deformation. Tests 3 and 4 followed this procedure from permanent deformations of 30 mm (Test 3) and 53.3 mm (Test 4) to peak deformations of 44.5 mm and 63.5 mm, respectively. The results from the static experiments are presented in Section 4.2.

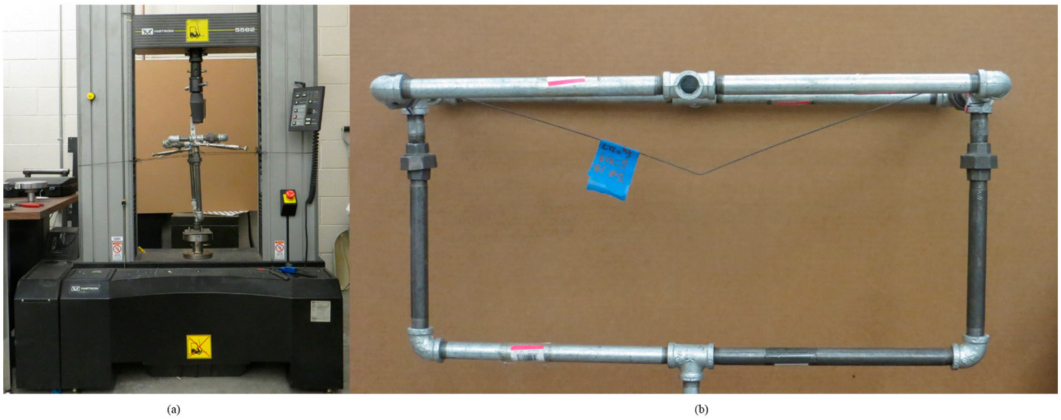

Figure 5. Experimental setup: (**a**) load frame, (**b**) reaction frame and specimen.

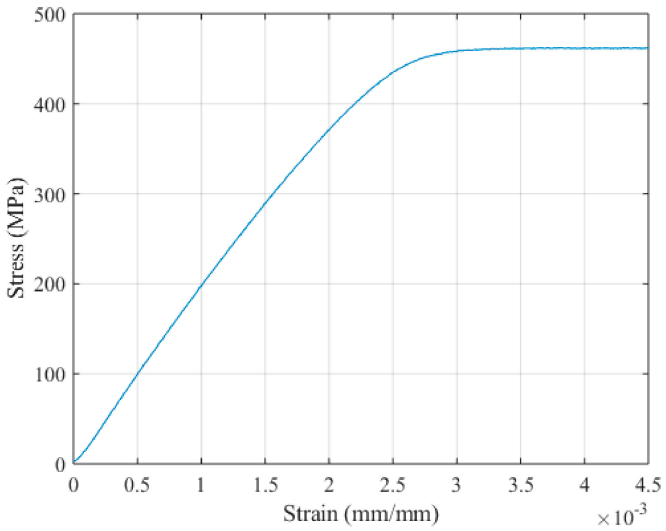

Figure 6. Stress–strain curve for Configuration 1 specimens.

3.3. Dynamic Experiments

Dynamic experiments performed on similar specimens were conducted to assess the dynamic behavior of modified catenary systems and to corroborate the analytical results. The same load frame used in previous tests was used to test specimens of similar geometry, span, and material properties. Loads of 9.81 N (1 kg) and 30.31 N (3 kg) were applied rapidly to illicit dynamic elastic and inelastic responses, respectively. Hanging masses of 1 kg and 3.1 kg were suspended in a position that lightly contacted the specimen, but imparted no significant force to the specimen. These loads were applied dynamically by burning the thin string supporting the hanging masses so they immediately transferred to the specimen in a free fall condition. Accelerations of each mass were measured using a single-axis micro–electrical–mechanical sensor (MEMS) accelerometer (Kistler KBeam 8315A) rigidly attached to the hanging mass. The results from the dynamic experiments are presented in Section 4.3.

4. Results and Discussion

4.1. Analytical Results

The first analysis includes determination of static and dynamic behavior predicted by the M.C. model, O.S. finite element results, and the approximate M.C. model for a fully defined cable subject to several loads. Figure 7 displays static and dynamic load-displacement curves for Configuration 2 in Table 1. Figure 7 shows the results of the static load deflection results for the M.C. model (Equation (5)), O.S., and the approximate M.C. model (Equation (9)); dynamic results are shown for discrete loading values for the M.C. model (Equation (5)), O.S., and the approximate M.C. model using the load amplification factors (Equation (10)). M.C. and O.S. results match exactly, and the approximate M.C. model matches well in the elastic range and begins to diverge as displacements increase in the inelastic range, with Equation (9) overestimating the load for a given deflection.

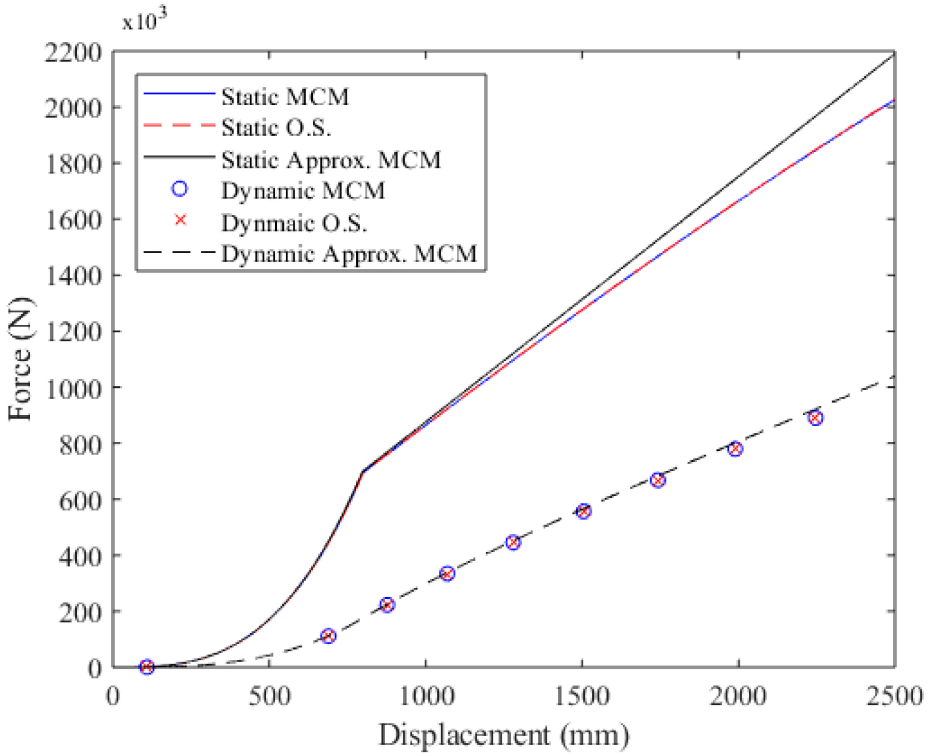

Figure 7. Analytical load-deflection results. MCM—modified catenary model. O.S.—OpenSees.

4.2. Static Experiment Results

Figure 8 displays load-displacement curves for four experimental tests shown as solid, continuous curves; analytical estimates of the response are overlaid with the dotted curves. Excellent agreement was observed between individual experimental tests and the analytical curves from the modified catenary model. The initial loading branch of each curve is increasingly linear as initial deflections increase as predicted by the modified catenary model.

Small variations between the predicted and observed response occur during the initial loading and near the yield point during Test 1; this behavior was observed in all static tests. The experimental data suggests that the specimen is slightly stiffer as it is initially loaded and is slightly more flexible near the end of the elastic phase. This is attributed to two primary sources of error: the inability to test a perfectly straight wire and the small pretensioning of the specimen during clamping. Small bends or imperfections in the specimen alter the unloaded length of each catenary leg and create very small amounts of slack that appear in the results as a softening of the curve. Pretensioning in the specimen

manifests as a stiffening of the curve. In the inelastic range, the model predicts a slightly stiffer curve; small flexibilities within the load frame and the support frame may attribute to this small discrepancy. At the scale considered in Configuration 1, small variations or uncertainties along a wire's cross-sectional area (1.4 mm to 1.6 mm), initial deflection (0 mm to 10 mm), and pretensioning (0 N to 22 N) contribute to experimental error.

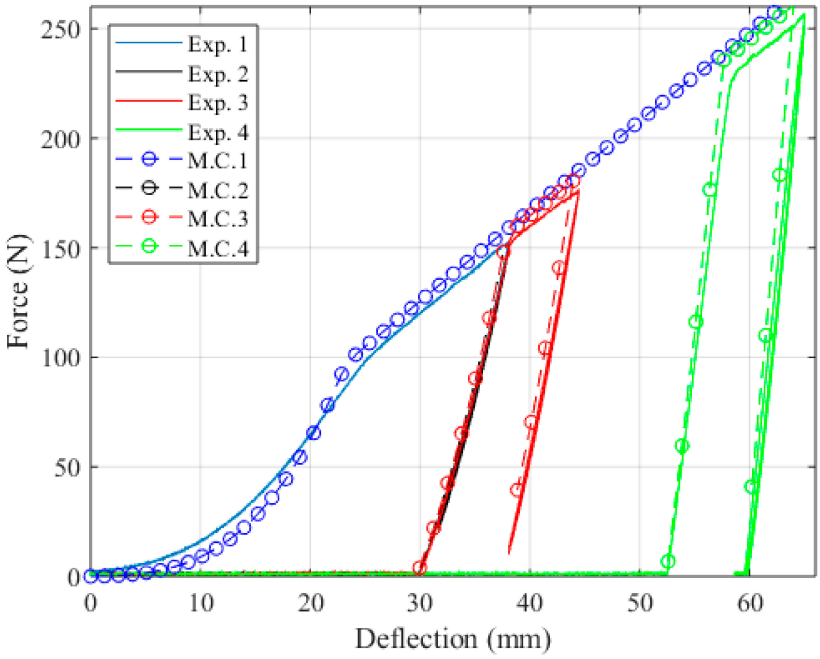

Figure 8. Static experimental results. Exp.—experiment.

4.3. Dynamic Experiment Results

Table 2 displays the results for ten dynamic tests performed on a total of five specimens. All five elastic tests were performed with individual specimens and applied loads of 9.8 N; inelastic tests were performed on the same five specimens with an applied load of 30.3 N. All specimens exhibited the same material behavior as the static specimens. The only variation in elastic experiments was the initial displacement, δ_0. Natural frequencies, natural periods, maximum and minimum accelerations for experiments (Exp.) and the modified catenary model (M.C.), and displacements for the modified catenary model (M.C.) are provided.

Table 2. Dynamic results of modified catenary experiments. M.C.—modified catenary model; Exp.—experiment.

Test	δ_0 (mm)	f_n (Hz)		T_n (s)		a^+ (g)		a^- (g)		u^+ (mm)	u^- (mm)
		M.C.	Exp.	M.C.	Exp.	M.C.	Exp.	M.C.	Exp.	M.C.	M.C.
Elastic 1	−1.50	7.99	8.90	0.13	0.11	2.62	3.05	−1.00	−1.03	−1.50	−15.88
Elastic 2	−0.29	7.99	8.40	0.13	0.12	2.81	1.88	−1.01	−1.10	−0.29	−16.11
Elastic 3	−0.50	7.99	7.95	0.13	0.13	2.76	1.60	−1.00	−0.96	−0.50	−16.04
Elastic 4	−1.81	7.99	9.05	0.13	0.11	2.49	2.66	−1.00	−1.10	−1.81	−15.71
Elastic 5	−1.61	7.99	7.60	0.13	0.13	2.52	1.70	−1.00	−0.89	−1.61	−15.75
Inelastic 1	−3.80	6.99	7.45	0.14	0.13	1.90	1.77	−1.03	−1.56	−3.80	−23.03
Inelastic 2	−0.41	7.99	8.45	0.13	0.12	2.05	1.50	−1.13	−1.10	−0.41	−24.24
Inelastic 3	−0.25	7.99	8.65	0.13	0.12	2.06	1.37	−1.13	−1.20	−0.25	−24.32
Inelastic 4	−6.60	6.99	7.35	0.14	0.14	1.84	1.64	−1.00	−1.31	−6.60	−22.54
Inelastic 5	−1.61	6.99	6.95	0.14	0.14	1.99	1.82	−1.08	−0.98	−1.61	−23.72

Figure 9 contains acceleration time histories from the dynamic M.C. and O.S. analyses, along with the measured acceleration from corresponding laboratory experiments. The trends in behavior of the experimental acceleration time histories match well with the modified catenary model for both the elastic and inelastic cases. Numerical values for analytical and experimental natural frequencies and periods in Table 2 also show strong correlations. Predicted frequencies for the elastic models were all approximately 8 Hz, while observed frequencies ranged from 7.6 Hz to 9.05 Hz. For the inelastic models, the calculated frequencies decreased to 7 Hz for specimens with larger initial deflections of 1.61 mm–6.6 mm. The observed natural frequencies for these specimens were the lowest observed frequencies of 6.95 Hz–7.35 Hz. While the time histories do show excellent shape agreement, specific magnitudes of acceleration vary from model to experiment. Initial deflections, load application, and material properties are uncertain quantities that were measured or estimated and characterized in the dynamic analyses, but errors in the experimental data can be attributed to these uncertainties.

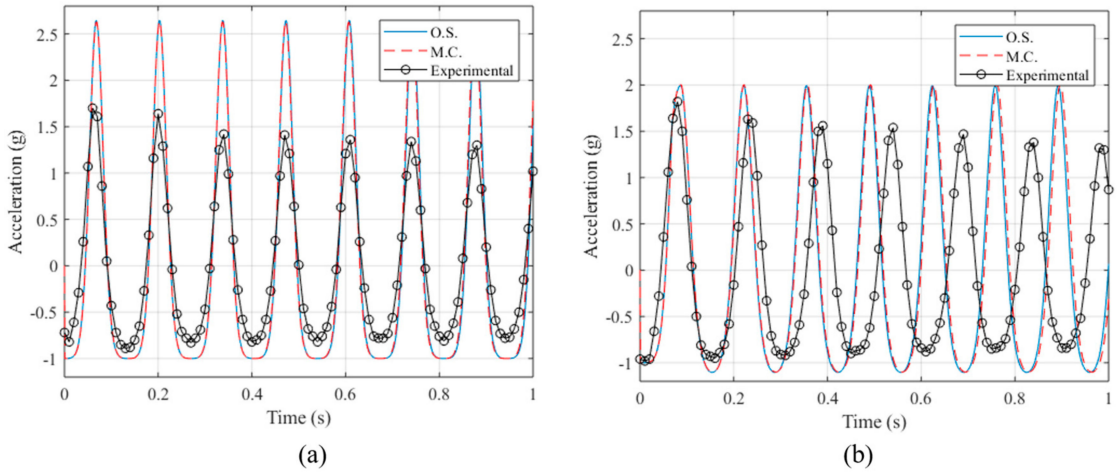

Figure 9. Dynamic experimental results: (**a**) elastic and (**b**) inelastic.

5. Application to Retrofit Cable Design

In practice, the design of retrofit cables for progressive collapse entails many considerations such as cable type, material properties, cross-section, and connection detailing. This paper provides a framework for the rational selection of cross-sectional area for retrofit cables to arrest motion and prevent progressive collapse. Equations for cross-sectional area are developed that meet two criteria for a selected cable type: (1) sufficient strength to arrest motion from a large, concentrated dynamic force; and (2) sufficient stiffness such that some arbitrary limiting deflection is not exceeded. The dynamically applied load is simply the factored design load calculated at the onset of the design problem; the deflection criteria is also dictated by the appropriate provision and might be chosen based on limiting strain, serviceability, or story height.

5.1. Retrofit Design Equations and Procedures

For a given required load, P_u, and a desired limiting deflection, αu_y, an adequate cable cross-sectional area can be determined by manipulating Equations (11) and (12) in the elastic and inelastic ranges, respectively. For elastic limiting deflections, the required area is as follows:

$$A_E = \frac{4P_u S^3}{E u_{SE}^3} \tag{21}$$

For the more likely scenario of the limiting deflection falling within the inelastic range, the required area becomes the following:

$$A_I = \frac{P_u \alpha^2}{\left(\alpha^2 - \frac{1}{2}\right) F_y u_{SI}} \tag{22}$$

The procedure for calculating the required area is as follows:

- Establish a given deflection limit, u_E or u_I (e.g., u_y, floor-to-floor height, ultimate strain)
- Calculate α from a given deflection limit and u_y from Equation (17)
- If $\alpha < 1$, use Equation (21), and if $\alpha > 1$, use Equation (22).

5.2. Illustrative Cable Retrofit Behavior Deisgn Example

In this example, two plausible design scenarios are illustrated. In both cases, the design load is 450×10^3 N and all geometric and material properties are provided in Configuration 2 of Table 2; the required cross-sectional area is the unknown variable to be designed. The two scenarios limit deflection by (1) onset of yield in the cable and (2) ultimate strain in the cable.

- Case 1

The deflection limit is equal to the deflection at yield, u_y. Using Equation (17), $u_y = 798$ mm. In this case, $\alpha = 1$, and either Equation (21) or Equation (22) may be used. The required area is 0.0083 mm^2.

- Case 2

The deflection limit is equal to the deflection at fracture, u_f. Assuming that the ultimate strain is approximately 0.04 and using Equation (4), $u_f = 1700$ and $\alpha = 2.2$ In this case, $\alpha > 1$, and Equation (22) leads to the required area of 0.0021 mm^2.

5.3. Limitations of the Method

This framework is not intended to serve as a codified procedure, but rather as a guideline to be used in the development of codified procedures as other research addresses additional design considerations. The equations and relationships developed in this work apply only to systems or system components that satisfy, or approximately satisfy, the assumptions outlined in Section 2. Specifically, the equations should only be applied to system components with negligible flexural resistance (including at the boundary conditions), concentrated mass at midspan, and equal spans. The model also considers an elastic–perfectly plastic constitutive relationship. Retrofit cables can meet these requirements, but other structural systems require further study to assess the effect of assumption violations on the M.C. model. Such candidate systems include the following: braced frames with shear tab connections; moment resisting steel frames, which may have their own flexural-catenary resistance; reinforced concrete frames in which the reinforcing steel serves as catenary resistance; and column supports that are not constrained horizontally or vertically.

6. Summary and Conclusions

The modified catenary model presented in this paper is an efficient, applicable tool that can be used to understand the fundamental mechanisms present in catenary scenarios in which mass is lumped to a central position and flexural resistance is small. This model follows from first principles and provides an efficient means to perform geometrically- and materially-nonlinear static or dynamic analyses. The following conclusions are based on research presented in this paper:

- As expressed in Equation (11), geometric nonlinearities in modified catenary systems in the elastic material range result in load carrying capacity that is approximately proportional to the cubic displacement.

- As expressed in Equation (12), geometric nonlinearities in modified catenary systems provide significant post-yield load carrying capacity that is approximately proportional to post-yield displacement.
- For a given displacement, the ratio of dynamic load to static load is ¼ for the elastic case and varies with α^2 post yield.
- Static and dynamic experimental results verify the applicability of modified catenary behavior for scaled cable systems (i.e., 16-gage steel wire with 680 mm spans).
- The approximate modified catenary equations adequately represent the essential features of a retrofit cable system and provide closed-form estimations of required cross-sectional areas to be used in design.

Author Contributions: L.T.D. and B.A.S. conceived and designed the experiments; L.T.D. performed the experiments; L.T.D. and Y.Z. analyzed the data; Y.Z. contributed the finite element modeling; L.T.D., Y.Z. and B.A.S. wrote the paper.

Funding: The authors greatly acknowledge the financial support provided by the Sam Taylor Fellowship award.

Conflicts of Interest: The authors declare no conflict of interest.

References

1. Yang, B.; Tan, K. Robustness of bolted-angle connections against progressive collapse: Experimental tests of beam-column joints and development of component-based models. *J. Struct. Eng.* **2013**, *139*, 1498–1514. [CrossRef]
2. Yu, J.; Rinder, T.; Stolz, A.; Tan, K.; Riedel, W. Dynamic progressive collapse of an RC assemblage induced by contact detonation. *J. Struct. Eng.* **2014**, 140. [CrossRef]
3. Orton, S.; Kirby, J. Dynamic response of a RC frame under column removal. *J. Perform. Constr. Facil.* **2014**, *28*, 04014010. [CrossRef]
4. Lee, C.H.; Kim, S.; Han, K.H.; Lee, K. Simplified nonlinear progressive collapse of welded steel. *J. Constr. Steel Res.* **2009**, *65*, 1130–1137. [CrossRef]
5. Alashker, Y.; Li, H.H.; El-Tawail, S. Approximations in progressive collapse modeling. *J. Struct. Eng.* **2011**, *136*, 914–924. [CrossRef]
6. Izzuddin, B.A. A simplified model for axially restrained beams subject to extreme loading. *Int. J. Steel Struct.* **2005**, *5*, 421–441.
7. Faridmehr, I.; Osman, M.H.; Tahir, M.M.; Nejad, A.F.; Azimi, M. Seismic and progressive collapse assessment of new proposed steel connection. *Adv. Struct. Eng.* **2015**, *18*, 439–452. [CrossRef]
8. Alp, Y. Combined Flexural and Cable-Like Behavior of Ductile Steel Beams. Master's Thesis, Auburn University, Auburn, AL, USA, 2009.
9. Livingston, E.; Sasani, M.; Bazan, M.; Sagiroglu, S. Progressive collapse resistance of RC beams. *Eng. Struct.* **2015**, *95*, 61–70. [CrossRef]
10. Fascetti, A.; Kunnath, S.K.; Nistico, N. Robustness evaluation of RC frame buildings to progressive collapse. *Eng. Struc.* **2015**, *86*, 242–249. [CrossRef]
11. Yi, L.; Lu, X.; Guan, H.; Ye, L.P. Progressive collapse resistance demand of reinforced concrete frames under catenary mechanism. *ACI Struct. J.* **2014**, *111*, 1225–1234.
12. Valipour, H.R.; Foster, S.J. Finite element modelling of reinforced concrete framed structures including catenary action. *Comp. Struct.* **2010**, *88*, 528–538. [CrossRef]
13. Stylianidis, P.M.; Nethercot, D.A.; Izzuddin, B.A.; Alghazouli, A.Y. Modelling of beam response for progressive collapse alanlysis. *Structures* **2015**, *3*, 137–152. [CrossRef]
14. Qian, K.; Li, B. Research advances in design of structures to resist progressive collapse. *J. Perform. Constr. Facil.* **2015**, 29. [CrossRef]
15. Qian, K.; Li, B.; Ma, J. Load-carrying mechanism to resist progressive collapse of RC buildings. *J. Struct. Eng.* **2015**, 141. [CrossRef]
16. Quiel, S.; Marjanishvili, S.; Katz, B. Performance-based framework for quantifying structural resilience to blast-induced damage. *J. Struct. Eng.* **2016**, 142. [CrossRef]
17. Weigand, J.; Berman, J. Integrity of steel single plate shear connections subjected to simulated column removal. *J. Struct. Eng.* **2014**, 140. [CrossRef]

18. Jian, H.; Zheng, Y. Simplified models of progressive collapse response and progressive collapse-resisting capacity curve of RC beam-column substructures. *J. Perform. Constr. Facil.* **2014**, 28. [CrossRef]
19. Yi, W.J.; He, Q.F.; Xiao, Y.; Kunnath, S.K. Experimental study on progressive collapse-resistant behavior of reinforced concrete frame structures. *ACI Struct. J.* **2008**, *105*, 433–439.
20. Yu, J.; Tan, K. Experimental and numerical investigation on progressive collapse resistance of reinforced concrete beam column sub-assemblages. *Eng. Struct.* **2013**, *55*, 90–106. [CrossRef]
21. Sasani, M.; Bazan, M.; Sagiroglu, S. Experimental and analytical progressive collapse evaluation of actual reinforced concrete structure. *ACI Struct. J.* **2007**, *104*, 731–739.
22. Tian, Y.; Su, Y. Dynamic response of reinforced concrete beams following instantaneous removal of a bearing column. *Int. J. Concr. Struct. Mat.* **2011**, *5*, 19–28. [CrossRef]
23. Smilowitz, T.; Tennant, D. Multi-hazard design to resist progressive collapse. In Proceedings of the 2001 Structures Congress, Washington, DC, USA, 21–23 May 2001.
24. Galal, K.; El-Sawy, T. Effect of retrofit strategies on mitigating progressive collapse of steel frame structures. *J. Constr. Steel Res.* **2010**, *66*, 520–531. [CrossRef]
25. Wu, T.X.; Brennan, M.J. Basic analytical study of pantograph-catenary system dynamics. *Veh. Syst. Dyn. Int. J. Veh. Mech. Mobil.* **1998**, *30*, 443–456. [CrossRef]
26. Wu, T.X.; Brennan, M.J. Dynamic stiffness of a railway overhead wire system and its effect on pantograph-catenary system dynamics. *J. Sound Vib.* **1999**, *219*, 483–502. [CrossRef]
27. Krishnasamy, S.; Kulendran, S. Combined wind and ice loads from historical extreme wind and ice data. *Atmos. Res.* **1998**, *46*, 123–129. [CrossRef]
28. American Society of Civil Engineers (ASCE). Minimum Design Loads for Buildings and Other Structures. In *ASCE/SEI 7-10*; American Society of Civil Engineers: Reston, VA, USA, 2013; ISBN 9780784412916.
29. Abdollahzadeh, G.; Mashmouli, M. Use of steel tendons in designing progressive collapse-resistant reinforced concrete frames. *J. Perfom. Constr. Facil.* **2017**, *31*, 04017023. [CrossRef]
30. Tan, S.; Astaneh-Asl, A. Use of steel cables to prevent progressive collapse of existing buildings. In Proceedings of the 6th Conference on Tall Buildings in Seismic Regions, Los Angeles, CA, USA, 4 June 2003.
31. Deputy, L.T.; Story, B.A. Progressive collapse mitigation: Geometrically nonlinear catenary behavior. In Proceedings of the Architectural Engineering Institute Conference, Milwaukee, WI, USA, 24–27 March 2015.
32. Kunnath, S.K.; Bao, Y.; El-Tawil, S. Advances in computational simulation of gravity-induced disproportionate collapse of RC frame buildings. *J. Struct Eng.* **2017**. [CrossRef]
33. Izzudin, B.A.; Vlassis, A.G.; Elghazouli, A.Y.; Nethrecot, D.A. Progressive collapse of multistory buildings due to sudden column loss. *Eng. Struct.* **2008**, *30*, 1308–1318. [CrossRef]
34. Dusenberry, D.; Hamburger, R. Practical means for energy-based analysis of disproportionate collapse potential. *J. Perform. Constr. Facil.* **2006**, 336–348. [CrossRef]
35. Xu, G.; Ellingwood, B.R. An energy-based partial pushdown analysis procedure for assessment of disproportionate collapse potential. *J. Constr. Steel Res.* **2011**, *67*, 547–555. [CrossRef]